K. J. Miller, H. J. Mohamed,* and E. R. de los Rios**

Fatigue Damage Accumulation Above and Below the Fatigue Limit

REFERENCE Miller, K. J., Mohamed, H. J., and de los Rios, E. R., **Fatigue Damage Accumulation Above and Below the Fatigue Limit**, *The Behaviour of Short Fatigue Cracks*, EGF Pub. 1 (Edited by K. J. Miller and E. R. de los Rios) 1986, Mechanical Engineering Publications, London, pp. 491–511.

ABSTRACT Damage accumulation in fatigue, initially incorporating cycles at stresses below the fatigue limit, was investigated in continuously increasing shear stress amplitude tests on a fully annealed 0.4 per cent carbon steel. Surface damage was observed throughout the test using a plastic replica technique. Fatigue cracks were observed at preferential sites coincident with persistent slip bands at stresses of the order of 85 per cent of the fatigue limit stress. Predictions of fatigue life based on classical models due to Palmgren–Miner, Corten–Dolan, and Marsh are shown to be non-conservative for increasing stress amplitude situations starting from stress levels below the fatigue limit. Satisfactory predictions are obtained, however, by combining crack growth rate expressions derived for short and long cracks. It is shown that a distinction must be made between the accumulation of fatigue damage in the short crack region and that in the long crack region if accurate life predictions are to be obtained. Damage accumulation at stress levels below the fatigue limit can have a significant effect on subsequent damage accumulation above the fatigue limit.

Notation

a	Surface crack length
a_f	Failure crack length
a_o	Initial surface roughness
a_t	Transition length between short and long cracks
d	Microstructure length parameter
A, B, C, m, n	Constants
N	Number of cycles
N_f	Number of cycles to failure in constant amplitude tests
N_{ff}	Number of cycles to failure in increasing stress amplitude tests
N_L	Number of cycles in the long crack growth phase
N_S	Number of cycles in the short crack growth phase
z	Slope of an hypothetical S–N curve
α	Increase in stress amplitude per cycle
$\Delta\gamma_p$	Plastic shear strain range
τ	Shear stress amplitude
ϕ	Increase in plastic shear strain range per cycle

* Mechanical Engineering Department, University of Sheffield, Mappin Street, Sheffield S1 3JD, UK.

Subscripts

CDM	Corten–Dolan–Marsh
f	Failure
i	Intermediate
FL	Fatigue limit
o	Initial
PM	Palmgren–Miner

Introduction

Possibly the earliest realization that fatigue damage could develop below the fatigue limit came about by examining laboratory specimens and machine elements operating at stresses in the vicinity of the fatigue limit. Non-propagating cracks generated at stress levels below the fatigue limit at geometrical discontinuities would be but one example (**1**). These and similar findings generated much laboratory research involving tests which tried to simulate practical conditions, i.e., two-step and multi-step stress levels with sudden or gradually increasing or decreasing changes in the stress level.

The most simple and popular criterion adopted for the analysis of results from such tests was the Palmgren–Miner hypothesis (**2**)(**3**) which is expressed as

$$\sum (N/N_f)_i = 1 \qquad (1)$$

Despite its popularity this hypothesis has two major shortcomings. First it assumes that damage accumulates in the same manner at all stress levels which implies that the mechanism of damage is unchanged throughout lifetime. However, by testing at one stress level for a certain number of cycles and then changing to a higher stress level for the remaining portion of the specimen's life, it has been shown that the summation expressed by the left-hand side of equation (1) is greater than unity because the accumulation of damage at low stress levels is much slower than at high levels (**4**)–(**6**) and involves different mechanisms. The second major shortcoming is the failure of equation (1) to consider damage in the form of cracking below the fatigue limit. In a variable stress range situation where some of the cycles are at a stress level below the fatigue limit (and hence N_f is necessarily infinite) the experimental summation term will be less than unity which indicates that a prediction of life based on the Palmgren–Miner hypothesis is dangerously optimistic.

To obviate these and other difficulties and to predict more accurately the life of a specimen or component that is subjected to a loading sequence involving some cycles at stress levels below the fatigue limit, some investigators have used a modified Palmgren–Miner rule based on a S–N curve derived from two-stress-level, single-block fatigue tests (**7**)(**8**). A similar approach had been introduced by Corten and Dolan (**9**) who proposed that such an S–N curve could be

determined from certain explicit assumptions on damage accumulation. Such a curve was shown to have a steeper slope than the constant stress amplitude S–N curve, but it apparently facilitated a more precise estimation of the contribution to fatigue damage at low stress ranges just above the fatigue limit.

Marsh (**10**) applied the Palmgren–Miner and the Corten–Dolan hypotheses to the results of fatigue tests in which stress cycles were contained within a symmetrical saw tooth envelope. While the former theory over-estimated the specimen life and erred by a factor of more than five in some cases, the latter theory agreed, at least qualitatively, with some of the experimental results. Further analysis showed that the Corten–Dolan prediction could be improved by considering cycles to be damaging at stress levels as low as 80 per cent of the fatigue limit. This new damaging limit, when used in conjunction with a linear summation rule, produced a more accurate life-prediction estimate.

This latter method does not identify or quantify damage accumulation below the fatigue limit. One aim of the present investigation is to study damage at stresses below the fatigue limit via a surface replication technique; damage being equated to the formation and growth of fatigue cracks. A second aim is to derive a model based on crack growth that can give accurate predictions of fatigue lifetime of plain specimens subjected to a continuously increasing stress amplitude and which incorporates stress levels below and above the fatigue limit.

Previous work

In a previous report (**11**) on the same material, a 0.4 per cent carbon steel, cracks were shown to form during constant amplitude tests at stresses below the fatigue limit; they grew to a certain length which was related to the extent of localized plasticity, usually of the order of a microstructural unit, and they were finally arrested at crystallographic barriers to plastic flow. According to the strength of the barrier the cracks were either temporarily or permanently arrested at the first barrier. Weak barriers were the ferrite grain boundaries while the pearlite regions were the strong impenetrable barriers. Nevertheless, eventual arrest was always attained at stresses below the fatigue limit. Some of these non-propagating or dormant cracks were seen to re-activate and continue to propagate as soon as the stress level was raised to a value higher than the fatigue limit.

Even at stresses above the fatigue limit an effect of the microstructure on crack growth rate was noticeable when the crack was small. In this short crack phase the growth rate showed a deceleration as the tip of the crack approached the microstructural barriers. This phase extended approximately to a crack length equivalent to the linear elastic fracture mechanics (LEFM) threshold. The following phase was the long crack region where crack growth was best characterized by an elastic–plastic fracture mechanics analysis.

Experimental details

The 0.4 per cent carbon steel used in the present investigation had a ferrite grain size which varied between 50 and 100 μm. The structure was banded and had a mixture of about 70/30 pearlite/ferrite. Full details of the heat treatment, microstructure, and specimen dimensions are given in reference (**11**). Fully reversed torsion fatigue tests were first carried out at constant shear stress amplitudes and then a series of tests were performed during which the shear stress amplitude was continuously and uniformly increased throughout a test until failure. The description of the machine and specimen calibration are given elsewhere (**12**). Plastic replicas were taken at specified intervals during tests on selected specimens. The replicas were subsequently observed, in the reverse order, in an optical microscope. The following information was thus obtained: number of cycles to the first sign of damage, number of cycles to the observation of cracks, crack length, crack orientation, and crack growth rate.

Constant amplitude tests

Constant amplitude tests at different shear stress amplitudes, τ, gave the results shown in Fig. 1. The data follow a linear relationship on a log–log plot up to the fatigue limit of $\tau = 122.5$ MPa with a confidence level of ± 2.27 MPa. Linear

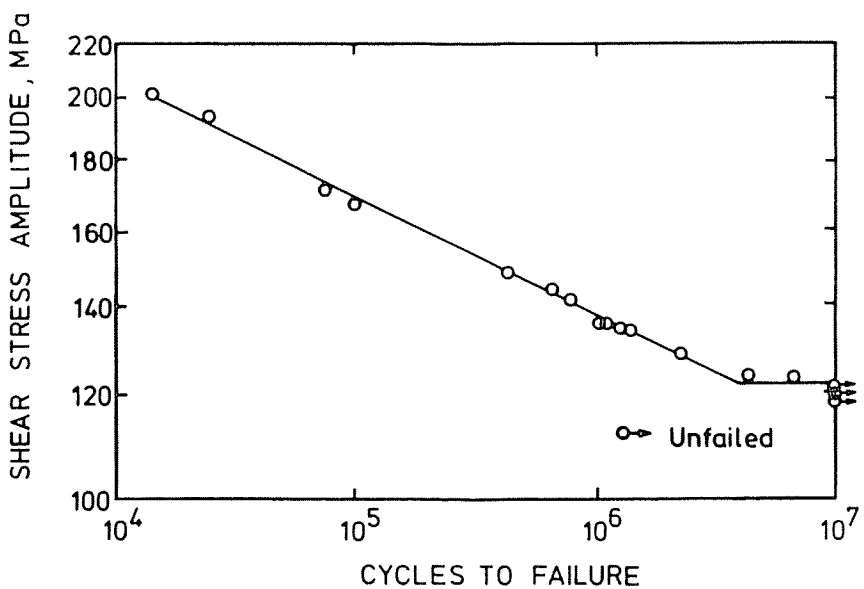

Fig 1 Constant stress amplitude fatigue life test data

regression analysis was used to find the best equation through the experimental points, i.e.

$$\tau = 429.57 N_f^{-0.08219} \tag{2}$$

Replicas taken from some of the specimens tested at different values of plastic strain range $\Delta\gamma_p$ allowed for the determination of the crack growth rate equations of the form presented by Miller (**13**) and Hobson (**14**). The equations which best fit the present experimental data are

$$\frac{da}{dN} = A(\Delta\gamma_p)^n(d - a); \quad \text{for short cracks} \tag{3}$$

with $A = 6$ and $n = 2.24$, and

$$\frac{da}{dN} = B(\Delta\gamma_p)^m a - C; \quad \text{for long cracks} \tag{4}$$

with $B = 17.4$, $m = 2.68$, and $C = 8.26 \times 10^{-4}$. In these expressions da/dN is given in μm/cycle.

Figure 2 shows the comparison of equations (**3**) and (**4**) with a set of experimental data. In the case of constant amplitude tests the value of d in equation (**3**) which best fits the data is 330 μm, which is of the same order of the crack length threshold, i.e., $a_{th} = 300$ μm, calculated for this material (**11**) from published values of ΔK_{th}. This value of 300–330 μm is the same as the average distance between the hard barriers of pearlite which are invariably separated in this banded structure by several grains of ferrite.

Increasing amplitude tests

In these tests a specimen is subjected to fatigue loading commencing at 0.7 of the fatigue limit stress, i.e., at a level sufficiently low where no damage is expected to be observed in a constant amplitude test (**11**); however, this initial stress amplitude continuously increases at a pre-determined rate, α, until failure.

By taking plastic replicas at intervals throughout the test a clear picture emerges of the initiation, type, and accumulation of damage. Figures 3 and 4 show two examples of a sequence of four replicas at various fractions of fatigue life for different values of α, one showing damage leading to a transverse crack, Fig. 3, the other leading to a longitudinal crack, Fig. 4. In both cases the sequence of events is the same, namely, the first sign of damage detected by this technique is the appearance of persistent slip bands (psbs) at approximately 0.15–0.3 of the fatigue life. Crack growth is only positively identified at about 0.85 of the fatigue limit stress amplitude. It is impossible to say which psbs will contain major cracks, because the plastic replica technique is not able to discern closed stage I, mode II cracks in single crystals, be they transverse or longitudinal cracks. At some stage the cracks break through into the adjacent grain

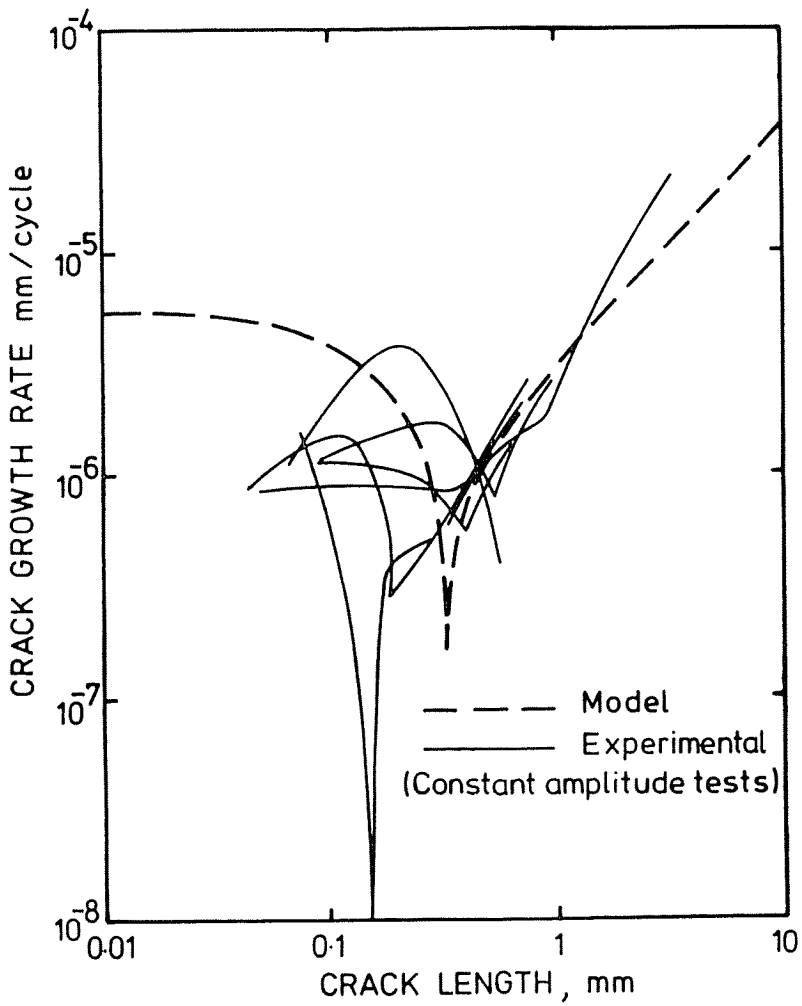

Fig 2 Experimentally determined surface crack growth rates at constant stress amplitude and predicted surface crack growth rates using equations (3) and (4)

and it is at this stage that the existence of a crack is certain and precise crack length measurements are possible. The early uncertainty as to the actual length of a closed stage I crack associated with a particular slip band is reflected by the symbols in Figs 5 and 6, which show psb and crack length measurements related to the fraction of fatigue life. With regard to the predictive model illustrated by the dashed curve, the assumption is that the crack that developed at the slip band in the first grain would propagate at a rate determined by equation (3) but

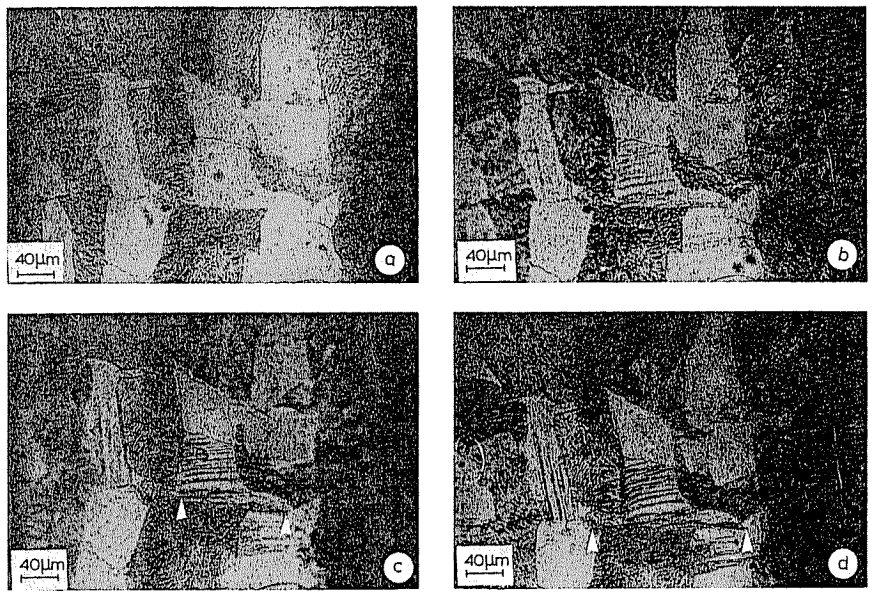

Fig 3 Replicas of fatigue damage and a transverse crack at various fractions of lifetime; N_{ff} = 1 477 500 cycles.
(a) $N/N_{ff} = 0$; $a = 0$ μm (b) $N/N_{ff} = 0.6$; $a = 112$ μm
(c) $N/N_{ff} = 0.8$; $a = 112$ μm (d) $N/N_{ff} = 0.9$; $a = 164$ μm

with the value of d now equal to 100 μm, since it is the largest ferrite grain which controls the development of the failure crack, especially at stresses below the fatigue limit (see later discussion).

In Fig. 5, at 0.28 N_{ff}, only psbs of various length are observed because the cracks are closed. As the stress amplitude increases it eventually attains, at 0.58 N_{ff}, a value of about 0.85 of the fatigue limit stress amplitude when several cracks are clearly discernible. In this test the fatigue limit stress amplitude is not reached until 0.78 N_{ff}, but considerable damage has already accumulated. Figure 6 shows similar characteristics, but because the rate of increase of stress amplitude is higher than in Fig. 5 there is a greater tendency for the crack development phases discussed previously to be accelerated. In subsequent theoretical calculations a failure surface crack length of 1.0 mm was assumed and Figs 5 and 6 show experimental life termination at 1.0 mm to permit comparisons between experiments and the model now to be discussed.

Life prediction methods and the crack growth model

Of the numerous methods published to assess cumulative damage in fatigue, two of the most popular methods will be applied to the result of the present

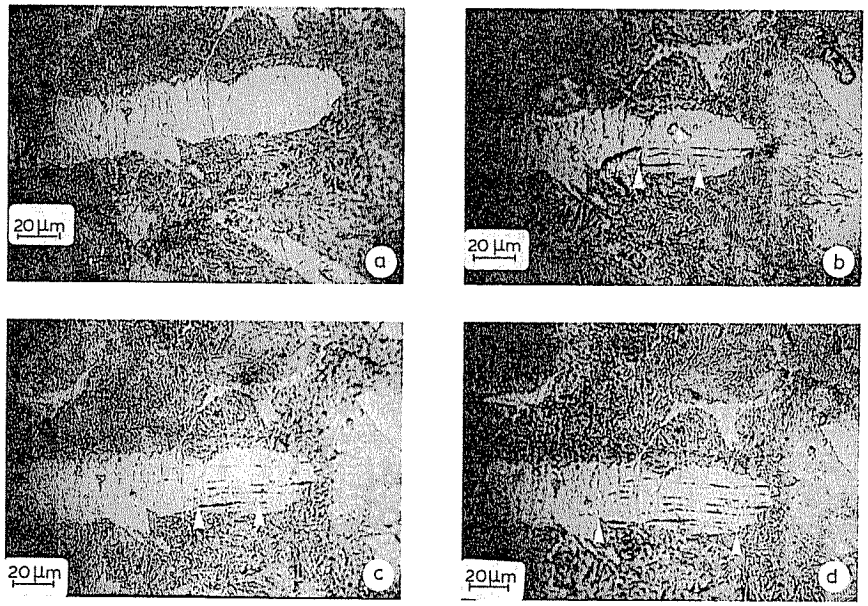

Fig 4 Replicas of fatigue damage and a longitudinal crack at various fractions of lifetime; $N_{ff} = 8\,964\,414$.
(a) $N/N_{ff} = 0$; $a = 0$ μm (b) $N/N_{ff} = 0.51$; $a = 30$ μm
(c) $N/N_{ff} = 0.57$; $a = 30$ μm (d) $N/N_{ff} = 0.62$; $a = 70$ μm

experiments. Finally a new method is derived based on the short and long crack growth rate expressions, equations (3) and (4). This method is compared with the two classical prediction methods and the experimental fatigue lifetime results.

The Palmgren–Miner hypothesis

Even though this hypothesis has been proved erroneous on several occasions, it is still in common use because of its simplicity. For complicated loading patterns or when a substantial part of the cycles are at stress levels below the fatigue limit, this hypothesis is known to frequently overestimate lifetime.

When applying the hypothesis to the continuously increasing load pattern of the present test, it can be shown (see Appendix A) that

$$\sum \left(\frac{N}{N_f}\right)_i = \frac{1}{\alpha} \int_{\tau_{FL}}^{\tau_f} \frac{1}{N_{f_i}} \, d\tau_i \qquad (5)$$

The integration of this equation requires an expression for N_f as a function of τ which can be obtained from constant amplitudes tests; see equation (2).

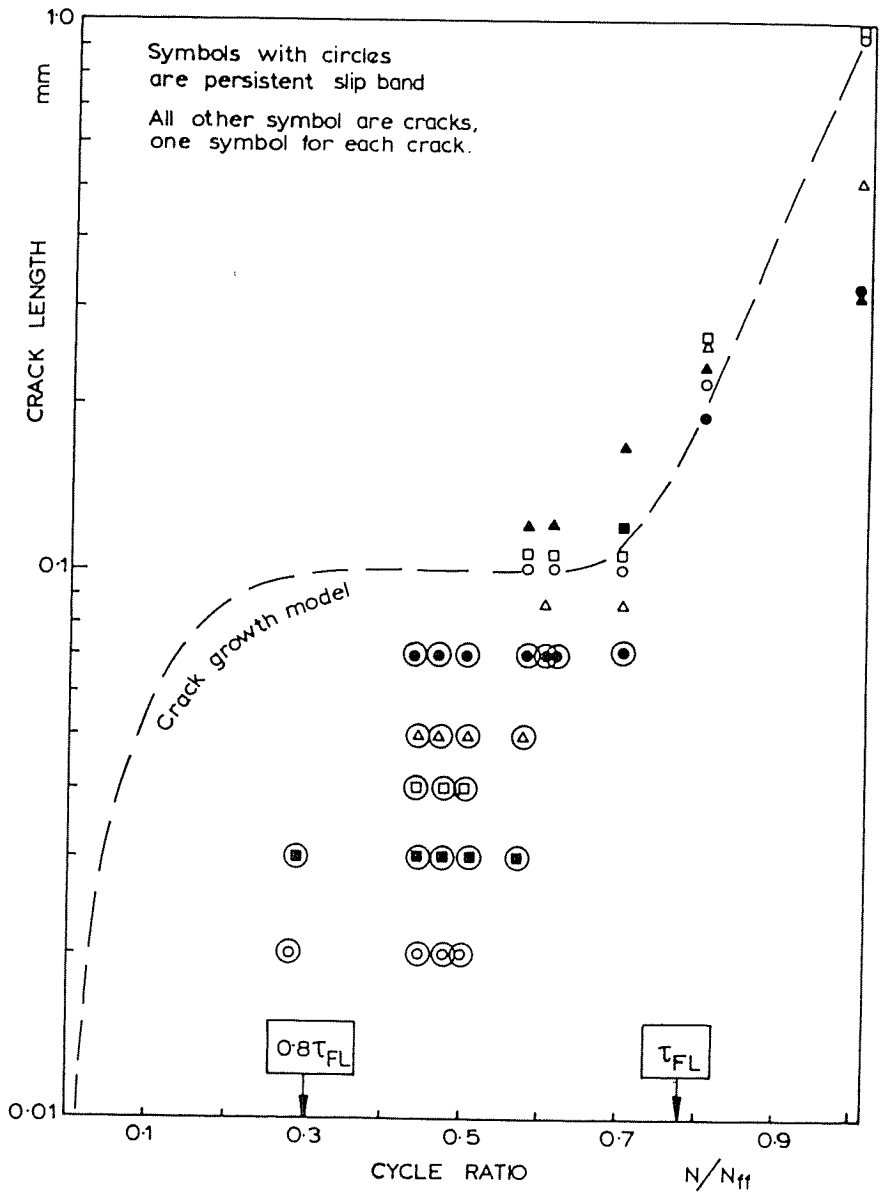

Fig 5 A typical fatigue damage versus fraction of fatigue life graph for one specimen: $N_{ff} = 8\,964\,414$; $\alpha = 5.687 \times 10^{-6}$ Nmm^{-2}/cycle. Different symbols identify different crack systems

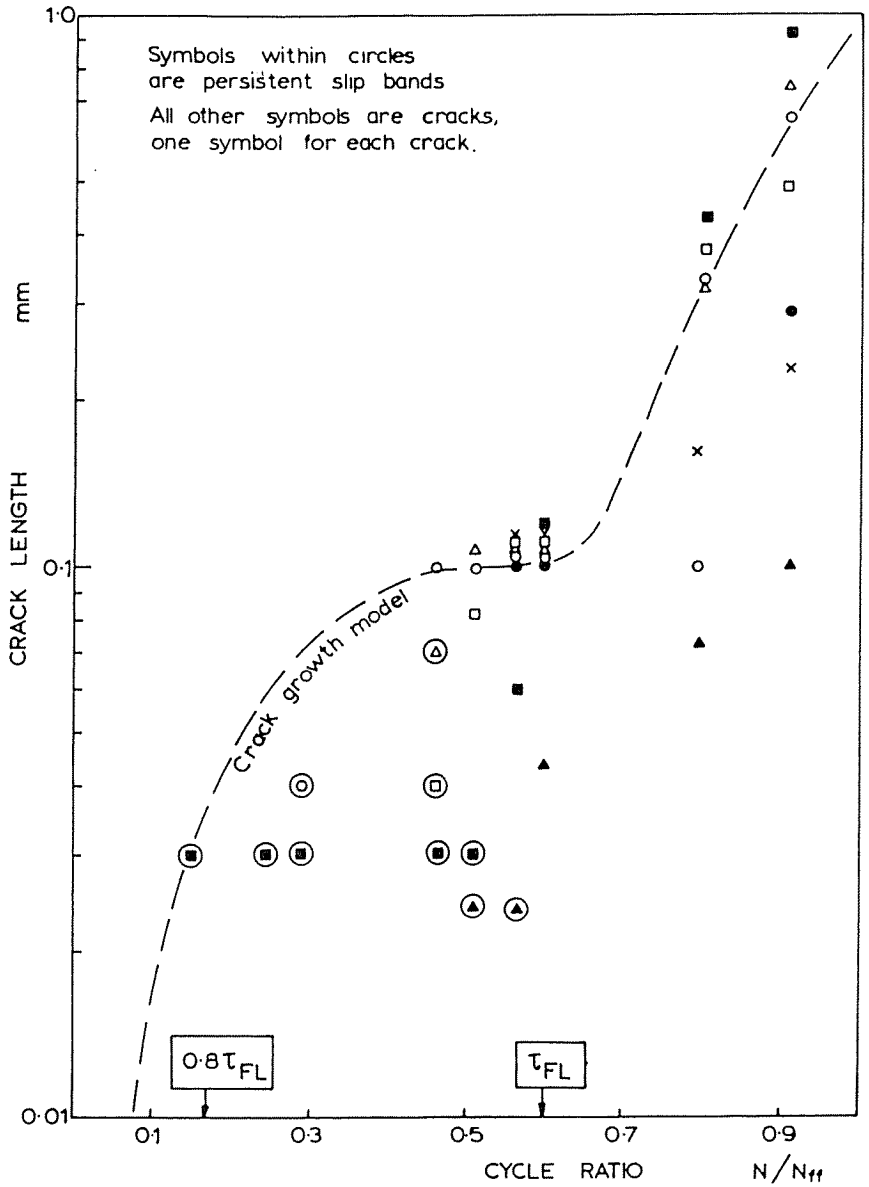

Fig 6 A typical fatigue damage versus fraction of fatigue life graph for one specimen: $N_{ff} = 1\,477\,500$; $\alpha = 3.808 \times 10^{-5}$ Nmm^{-2}/cycle. Different symbols identify different crack systems

Table 1 Fatigue lifetimes: predictions and experiment

Specimen	N_{ff} *Palmgren–Miner*	N_{ff} *Corten–Dolan–Marsh*	N_{ff} *from equations (3) and (4)*	N_{ff} *Expt*
1F	1 181 729	1 088 650	524 051	560 330
2D	2 665 370	2 327 891	856 412	981 485
3E	4 034 376	3 337 194	1 269 919	1 373 775
2X	4 958 005	3 978 989	1 474 681	1 477 500
2E	5 230 679	4 060 845	2 431 022	2 781 724
1E	9 848 154	6 720 333	4 873 670	8 964 414

Introducing this relation into equation (5) and making the summation equal unity, integrating and replacing α by the term $(\tau_f - \tau_o)/N_{ff}$, the predicted number of cycles to failure, N_{ff}, can be obtained from the expression

$$N_{ff}(\tau_f^{13.166} - \tau_{FL}^{13.166}) = 1.428 \times 10^{33}(\tau_f - \tau_o) \qquad (6)$$

From Fig. 1, the value of τ_{FL} is 122.5 MPa. Values of N_{ff} for six specimens are given in Table 1 and plotted in Fig. 7, as the Palmgren–Miner curve.

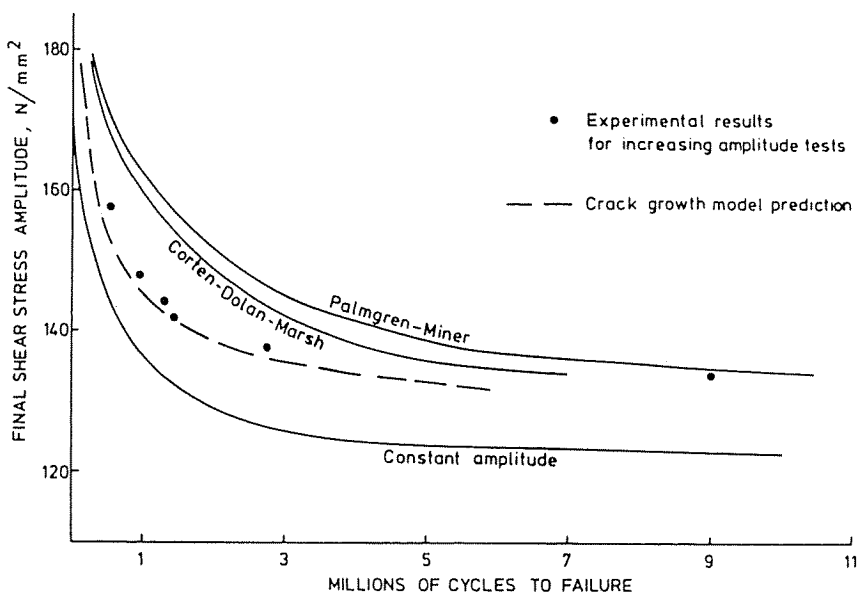

Fig 7 Increasing stress amplitude test results for different values of α, together with lifetime predictions from three models: (i) Palmgren–Miner, (ii) Corten–Dolan–Marsh, (iii) short and long crack growth rate equations

The Corten–Dolan–Marsh hypothesis

Corten–Dolan based their ideas on a theory of damage visualized as the nucleation of submicroscopic voids which developed into cracks, these cracks then propagated at a rate which depends on the stress level. The expression derived for multi-stress conditions was

$$N_g = N_h / \sum \beta_i \left(\frac{\sigma_i}{\sigma_h}\right)^z \tag{7}$$

where

N_g is the number of cycles to failure under a multi-stress programme
N_h is the number of cycles to failure at a constant stress amplitude, σ_h, equal to the highest stress achieved in the multi-stress test
β_i is the fraction of cycles at a stress level of σ_i
z is the inverse slope of an hypothetical log σ/log N relation which allows for the interaction effects of high and low stress levels

Marsh applied this expression to rotating–bending fatigue tests subjected to a triangular stress block and found that life predictions could be improved if stress cycles down to about 0.8 of the experimental fatigue limit were considered in the calculations. The new fatigue limit was interpreted as being that of the hypothetical S–N curve.

If the Corten–Dolan approach coupled with the developments due to Marsh is applied to the present experimental tests, the following expression is obtained (see Appendix A)

$$\frac{N_{ff}}{N_f} = \frac{(1 - y)(z + 1)}{1 - r^{z+1}} \tag{8}$$

In this expression

$$y = \tau_o/\tau_f \text{ and } r = 0.8\tau_{FL}/\tau_f$$

where

τ_o is the initial stress amplitude
τ_f is the final stress amplitude
$0.8\tau_{FL}$ is 80 per cent of the fatigue stress limit

In order to predict the number of cycles to failure, N_{ff}, a value of the hypothetical S–N curve inverse slope z has to be determined (see Appendix A).

Figure 7 and Table 1 show that the lifetime predictions using the Palmgren–Miner rule are dangerously non-conservative, overestimating the specimen life in some cases by a factor of two. The Corten–Dolan–Marsh method, which considers the interactive effects between high and low stress levels and also the damage from cycles below the fatigue limit stress down to a minimum level of $0.8\tau_{FL}$, gives a slightly better approximation; however the predictions are still non-conservative.

Fatigue life prediction from crack growth considerations

The main cause of error in both of the above mentioned classical methods is that they consider damage to accumulate according to a parabolic law of defect growth at both high and low stresses. It is now known that this presumption is not true; cracks less than a certain threshold length, a_{th}, propagate at an entirely different rate to cracks longer than α_{th}. For example, crack length measurements taken during constant stress amplitude tests lead to the development of the fundamentally different equations (3) and (4) for the short and long crack regions, respectively.

Since the variation of $\Delta\gamma_p$ with N is known for each test having an increasing amplitude of stress, equations (3) and (4) can be integrated to find the number of cycles in both the short and long crack stages; N_S and N_L, respectively. Their simple addition gives a predicted number of cycles to failure N_{ff}. The short crack region exends from $a_o \cong 0$ to a_t where a_t is the crack transition length between the short and long crack growth phases.

From equations (3) and (4) it is also possible to determine values of a_t, for situations in which the strain amplitude is increasing at a cyclic rate of ϕ from an initial plastic strain amplitude of $\Delta\gamma_{p_o}$. The equations for a_t, N_S, and N_L are simple to derive since, at a_t and N_S, the rate of growth da/dN for both the short and long cracks, are identical. However, the required equations are cumbersome and so are presented in Appendix B. Table 1 lists the values of the predicted life and Fig. 7 shows the same predictions in graphical form. The predictions using the crack growth equations are very close to the experimental fatigue lives while the two classical methods considered previously are non-conservative for the reasons already given. Figure 7 shows for comparative purposes the lifetime for constant amplitude tests which are reported in a separate publication (**15**) but it should be noted that this curve also is similarly and accurately predicted by combining the short and long crack growth equations with a tendency to slight conservatism.

Discussion

The Corten–Dolan–Marsh method shows an improvement when compared to the Palmgren–Miner method when predicting fatigue lives in situations of increasing stress amplitude cycles, but it is still a non-conservative method of prediction. The slight improvement of predictive capability via the Corten–Dolan hypothesis is due to account being taken of the interaction effect of low and high stresses (i.e., the switching to different deformation substructures at different stress levels) because crack growth rate depends on the flow stress which is a function of the substructure developed in the plastic zone. This stress history effect was introduced by Corten–Dolan by invoking a hypothetical S–N curve with a slope greater than the experimental one. The other factor which improves the prediction, as pointed out by Marsh, is defining a lower limit (80 per cent of the fatigue limit stress) for the initiation of damage. This is in

accordance with recent work showing that fatigue cracks can be initiated by cycling at stresses below the fatigue limit (**11**). The lower limit of $0.8\tau_{FL}$ is somewhat arbitrary and was obtained by Marsh to fit particular test data; no physical interpretation was attempted at that time.

The microstructural observations in the present work suggest that damage is initiated by the formation of persistent slip bands (psbs) in favourably orientated ferrite grains. The psbs are formed well before the applied stress approaches the level of the fatigue limit, in fact well developed psbs are observed even below the $0.8\tau_{FL}$ stress level; see Figs 5 and 6. How many of these slip bands contain significant cracks is impossible to say with the present experimental technique, but recent advances in acoustic microscopy (**16**) show great potential in the detection of very small closed cracks and it is expected that this new technique will provide valuable data. Nevertheless the plastic replica techniques will identify cracks as soon as they propagate into surrounding grains, although it should be noted that not all psbs are able to propagate a crack into the next grain. Limited quantitative information from these tests reveal that only between 5 and 10 per cent of psbs are able to extend cracks into neighbouring regions. As the stress approaches the level of the fatigue limit in an increasing amplitude test, coalescence of microcracks may take place and by the time cracks approach the critical size for long crack propagation only a very few cracks have attained a length that can propagate as long cracks to failure.

The dashed curves of Figs 5 and 6 show that the crack growth model tends to be the upper bound on observed damage and that, although cracks are only seen when they are about 50–100 μm in length, it is reasonable to assume that the psbs are disguising the presence of closed cracks in single grains. This is in sympathy with the hypothesis of Miller (**13**) that cracks grow immediately from the first cycle, but because they are initially smaller than psbs and are closed Stage I cracks they are exceedingly difficult to detect. It is also noticeable from Figs 5 and 6 that the higher the value of α (the cyclic rate of increase in stress amplitude) the closer are the two phases of crack growth; expressed another way there is a reduced tendency for cracks to decelerate.

Figure 7 shows that a much better prediction of lifetime is obtained if both the crack growth rate functions are available for the two main phases of crack growth – the short and the long crack regions. The method of prediction proposed here employs the two crack growth equation derived from experimental data obtained from constant amplitude tests. The short crack equation, equation (3), follows the model given by Miller (**13**) and Hobson (**14**) except that the plastic strain range is used to complement the long crack law, equation (4), as proposed by Miller and Ibrahim (**6**).

There is one major difference between the constant amplitude tests on the same material at stresses around the fatigue limit and the present series involving increasing stress amplitudes. In the former tests discussed in reference (**11**), the microstructural parameter, d, in equation (3) was of the order of the pearlite–pearlite distance (330 μm) and the short cracks only decelerated to

be arrested at those strong microstructural barriers. Alternatively one may say that the fatigue limit stress amplitude was always sufficiently high to quickly overcome the weaker barriers of the ferrite grain boundaries observed at lower stress levels. In the increasing amplitude tests, a considerable proportion of the lifetime was spent at relatively low stress levels at which even the ferrite grain boundaries provided sufficiently strong barriers to crack growth. Figures 5 and 6 indicate that at stress levels well below the fatigue limit the major barrier occurs at approximately 100 μm (i.e., the largest ferrite grain size) at about 60 per cent of lifetime; thereafter the crack accelerates and enters the long-crack growth phase given by equation (4). By the time the crack reaches a length of 300–330 μm (the average pearlite band separation distance) the applied stress level is above the fatigue limit and the pearlite barrier in this situation is not as effective as in a constant stress amplitude test equal to the fatigue limit stress level. This interesting phenomenon of stress level dependent barriers to crack growth will be discussed at some length in a future publication (**17**) and it is sufficient to report here that by equating d to the ferrite grain size in equation (3) a predictive model is derived that gives good correlation with the experiment data of Figs 5 and 6 and also a model that can be employed to give an excellent, slightly conservative estimate of fatigue lifetime as witnessed in Fig. 7.

In the present tests, therefore, the short crack region extends from a value of $a = a_o$ (the initial roughness) to a value of $a = a_t$ corresponding to a value at which the short and long crack growth rates are identical; values of a_t are given in Table B1 in Appendix B. The long crack region extends from $a = a_t$ to $a = a_f = 1.00$ mm, where a_f is the surface crack length at failure.

Finally, it appears from Fig. 7 that the entire lifetime of specimens is spent in propagating a crack from the first cycle, and that if any crack birth period exists it is negligible and can be omitted from lifetime calculations; a similar result to that given in reference (**13**). However, it appears that cracks can be arrested for a considerable period at strong barriers. In a recent paper (**18**) the temporary arrest of a short crack at a pearlite zone was shown to extend the fatigue lifetime by a factor varying linearly from one to two over fatigue lifetimes of one million to six million cycles, i.e., three million cycles were spent out of a total of six million cycles for the short crack to circumnavigate and/or cut through the pearlite.

Conclusions

(1) Classical fatigue life prediction methods, e.g., the Palmgren–Miner method or the Marsh modification to the Corten-Dolan method, are not satisfactory for predicting life in a continuously increasing stress amplitude situation due to their inability to take account of the complex crack growth behaviour of materials close to the fatigue limit where cracks decelerate before accelerating to failure.

(2) Fatigue damage is initiated well below the fatigue limit stress and can be observed as persistent slip bands (psbs) and microcracks. Few of these psbs contain cracks that can extend beyond the first grain.

(3) Two distinct equations for fatigue crack growth rate, one for the short crack phase and the other for the long crack phase, can be suitably combined to accurately predict the fatigue life of specimens tested at increasing stress amplitudes.

Appendix A: Calculation of damage summation terms

(1) *The Palmgren–Miner hypothesis applied to increasing stress amplitude tests*

For a linear increasing stress situation, the summation of damage requires to consider each cycle, hence

$$\sum \left(\frac{N}{N_f}\right)_i = \frac{N_1}{N_{f_1}} + \frac{N_2}{N_{f_2}} + \cdots \tag{A1}$$

where i = 1, 2, 3, . . . and N is one cycle.

Equation (A1) can be written in the form, $\sum (1/N_f)_i$ or, more generally

$$\int_{\tau_{FL}}^{\tau_f} \frac{1}{N_{f_i}}\, dx_i \tag{A2}$$

where

τ_{FL} is the fatigue limit stress obtained from constant amplitude tests
τ_f is the stress at failure during an increasing amplitude test
N_{f_i} is the fatigue life corresponding to τ_i

and, from a consideration of slopes in Fig. A1,

$$x_i = \frac{N_{ff}(\tau_i - \tau_o)}{(\tau_f - \tau_o)} \tag{A3}$$

where

N_{ff} is the number of cycles at failure for an increasing amplitude test, and
τ_o is the initial stress amplitude.

Differentiating equation (A3) and subsituting for dx_i in equation (A2) gives

$$\sum \left(\frac{1}{N_f}\right)_i = \int_{\tau_{FL}}^{\tau_f} \left(\frac{1}{N_f}\right)_i \frac{N_{ff}\, d\tau_i}{(\tau_f - \tau_o)} \tag{A4}$$

However, the rate of increase of stress, α, is a controlled test-variable and so equation (A4) can be summarized as

$$\sum \left(\frac{1}{N_f}\right)_i = \frac{1}{\alpha} \int_{\tau_{FL}}^{\tau_f} \frac{1}{N_{f_i}}\, d\tau_i \tag{A5}$$

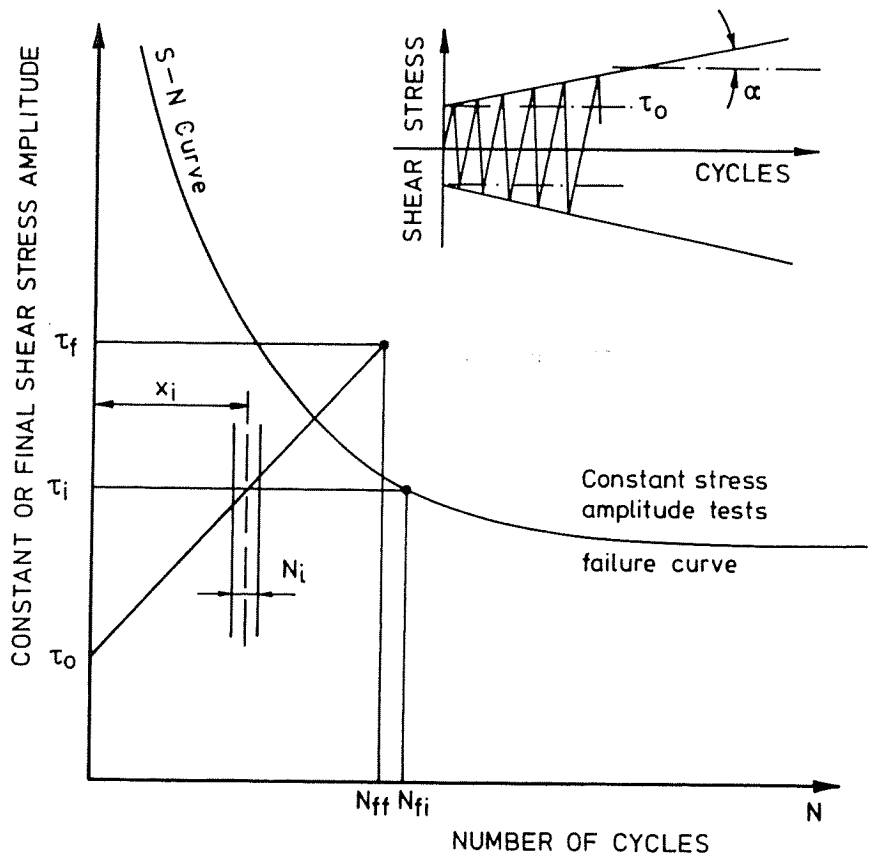

Fig A1 Schematic to illustrate experiment and model parameters

If the relationship between τ and N_f is known, i.e., the conventional S–N curve, the above equation can be integrated to give the required summation of damage according to Palmgren–Miner.

(2) *The Corten–Dolan–Marsh method applied to increasing amplitude tests*

Marsh (**10**) formulated an expression for the summation of fatigue damage, based on the work of Corten and Dolan (**9**), the latter leading to the prediction of the number of cycles to failure as

$$N_{ff} = \frac{N_f}{\sum \beta_i (\tau_i/\tau_f)^z} \tag{A6}$$

where

N_{ff} is the predicted life at failure for an increasing stress amplitude
N_f is the number of cycles to failure at constant stress amplitude, τ_f
β_i is the fraction of cycles at τ_i
z is an experimentally determined parameter

One of the conclusions that can be derived from the work of Marsh (**10**) is that the parameter z can be determined by making equation (A5) equal to unity and integrating it between the limits $0.8\tau_{FL}$ and τ_f in order to account for damage below the fatigue limit, hence

$$\sum \left(\frac{1}{N_f}\right)_i = \frac{1}{\alpha}\int_{0.8\tau_{FL}}^{\tau_f}\left(\frac{1}{N_f}\right)_i d\tau_i = 1 \qquad \text{(A7)}$$

This embodies the proposal of the hypothetical S–N curve, discussed previously in the main text, which can be described for the present tests as

$$\frac{1}{N_f} = \left(\frac{\tau}{429.57}\right)^z \qquad \text{(A8)}$$

Equation (A8) is similar to the conventional S–N curve equation but with a steeper slope.

Substituting (A8) into (A7) and integrating

$$1 = \left(\frac{1}{429.57}\right)^z \frac{1}{\alpha(z+1)}(\tau_f^{(z+1)} - 0.8\tau_{FL}^{(z+1)}) \qquad \text{(A9)}$$

If the stress rate, α, is known, the value of z can be obtained by iteration. In the present case the Newton–Raphson formula was used. Values of z for different α values are given in Table A1.

Now in equation (A6) β_i is equal to $d\tau_i/)\tau_f - \tau_o)$ and so the term

$$\sum \beta_i\left(\frac{\tau_i}{\tau_f}\right)^z = \int_{0.8\tau_{FL}}^{\tau_f}\frac{d\tau_i}{(\tau_f - \tau_o)}\left(\frac{\tau_i}{\tau_f}\right)^z$$

$$= \frac{\tau_f^{-z}}{(\tau_f - \tau_o)(z+1)}(\tau_f^{(z+1)} - 0.8\tau_{FL}^{(z+1)}) \qquad \text{(A10)}$$

From equation (A10) it follows that equation (A6) can be rewritten as

$$\frac{N_{ff}}{N_f} = \frac{(z+1)(1-y)}{1 - r^{z+1}} \qquad \text{(A11)}$$

where

$$r = \frac{0.8\tau_{FL}}{\tau_f};\quad y = \frac{\tau_o}{\tau_f};\quad z = 11.60, \text{ the average value in Table A1.}$$

It follows that if the conventional S–N curve and the stress at failure in an increasing amplitude test are known, then N_{ff} can be calculated from the above equation; this life prediction being based on the assumptions of the Corten–Dolan–Marsh theory of damage accumulation. The fraction N_{ff}/N_f is the summation of damage term which is always greater than unity.

Table A1

Specimen	α $(Nmm^{-2}/cycle)$	z
1F	1.232×10^{-4}	11.52
2D	6.348×10^{-5}	11.335
3E	3.85×10^{-5}	11.395
2X	3.808×10^{-5}	11.263
2E	1.825×10^{-5}	11.748
1E	5.687×10^{-6}	12.359

Appendix B: Derivation of equations to determine the lifetimes of the short and long crack growth phases

Experimental crack growth data obtained from constant amplitude tests are of the form

$$da/dN = A(\Delta\gamma_p)^n(d - a); \quad \text{for short cracks} \qquad \text{(B1)}$$

and

$$da/dN = B(\Delta\gamma_p)^m a - C; \quad \text{for long cracks} \qquad \text{(B2)}$$

Here

A, n, B, m, and C are material constants
a is the crack length
d is a microstructural parameter related to the distance between obstacles to crack growth
$\Delta\gamma_p$ is the plastic shear strain range

Equation (B1) is valid from a_o (surface roughness) to a_t, the crack transition length between the short and long crack growth phases.

In an increasing amplitude test the plastic strain range may be considered to vary approximately linearly with number of cycles, and so

$$\Delta\gamma_p = \Delta\gamma_{p_o} + \phi N \qquad \text{(B3)}$$

where

$\Delta\gamma_{po}$ is the initial plastic shear strain range
ϕ is the rate of increase of plastic shear strain range

Integrating equation (B1) and assuming a_o is approximately zero, since $a \approx 0 - 2\ \mu m$ has little effect on lifetime prediction (**13**)

$$\int_{a_o}^{a_t}\frac{da}{d-a} = A\int_o^{N_s}(\Delta\gamma_{po} + \phi N)^n\, dN$$

or

$$-\ln (1 - a_t/d) = A\left\{(\Delta\gamma p_o + \phi N)^{n+1}\right\}_o^{N_s}/(n + 1)\phi \quad \text{(B4)}$$

but since

$$\Delta\gamma_{p_s} = \Delta\gamma_{p_o} + \phi N_s \quad \text{(B5)}$$

where N_s is the number of cycles to complete the short crack propagation phase, then from equations (B4) and (B5)

$$\Delta\gamma_{p_s} = \{\Delta\gamma_{p_o}^{n+1} - (n + 1)\phi A^{-1} \ln (1 - a_t/d)\}^{1/(n+1)} \quad \text{(B6)}$$

Also when the crack length is equal to a_t then equation (B1) is equal to equation (B2), hence

$$a_t = \frac{Ad(\Delta\gamma_{p_s})^n + C}{A(\Delta\gamma_{p_s})^n + B(\Delta\gamma_{p_s})^m} \quad \text{(B7)}$$

When substituting (B6) into (B7), a value of a_t can be determined for a given rate of increase of plastic shear strain range ϕ, determined from experiment. The number of cycles for the short crack propagation phase, N_s, can then be obtained from equations (B5) and (B6) as

$$N_s = [\{\Delta\gamma_{p_o}^{n+1} - (n + 1)\phi A^{-1} \ln (1 - a_t/d)\}^{1/(n+1)} - \Delta\gamma_{p_o}]/\phi \quad \text{(B8)}$$

To predict the number of cycles corresponding to the long crack propagation phase, N_L equation (B2) can be integrated from a_t to a_f (here $a_f = 1000\ \mu m$). Assuming C = 0 for simplicity

$$\int_{a_t}^{a_f} \frac{da}{a} = \int_{N_S}^{N_S+N_L} B(\Delta\gamma_p)^m\, dN \quad \text{(B9)}$$

But

$$\Delta\gamma_p = \Delta\gamma_{p_s} + \phi(N - N_S) \quad \text{(B10)}$$

Substituting equation (B10) into equation (B9) and integrating

$$N_L = [\{\Delta\gamma_{p_s})^{m+1} + \phi(m + 1)B^{-1} \ln a_f/a_t\}^{1/(m+1)} - \Delta\gamma_{p_s}]/\phi \quad \text{(B11)}$$

Here $\Delta\gamma_{p_s}$ is determined from equation (B6).

Table B1

Specimen	$\phi \times 10^9$	a_f (μm)	N_S	N_L	$N_S + N_L$	N_{ff} *Expt*
1F	9.89	81.09	266 386	257 665	524 051	560 330
2D	4.76	90.36	463 366	393 046	856 412	981 485
3E	2.948	95.75	767 077	502 842	1 269 919	1 373 775
2X	2.188	98.039	900 952	573 729	1 474 681	1 477 500
2E	1.369	99.767	1 749 987	681 035	2 431 022	2 781 724
1E	0.3557	99.99	3 329 599	1 544 071	4 873 670	8 964 414

Table B1 gives values of N_S and N_L for various test conditions. The same table also gives values of a_t calculated by combining equations (B7) and (B6) and solving iteratively via a simple computer program.

The above data have not been reduced to three or four significant digits. They are either computed values or, in the case of experiments, data taken from the fatigue machine cycle counter.

Acknowledgements

Grateful thanks are extended to the Science and Engineering Research Council of the UK, Rio Tinto Zinc, and the Iraqi government for funding this programme of research.

References

(1) FROST, N. E., POOK, L. P., and MARSH, K. J. (1974) *Metal fatigue* (Clarendon Press, Oxford).
(2) PALMGREN, A. (1924) The fatigue life of ball bearings (in German) *ZVDI*, **68**, 339–341.
(3) MINER, M. A. (1945) Cumulative damage in fatigue, *J. Appl. Mech.*, **12**, A159–A164.
(4) MILLER, K. J. and ZACHARIAH, K. P. (1977) Cumulative damage laws for fatigue crack initiation and stage I propagation, *J. Strain Analysis*, **12**, 262–270.
(5) IBRAHIM, M. F. E. and MILLER, K. J. (1980) Determination of fatigue crack initiation life, *Fatigue Engng Mater. Structures*, **2**, 351–360.
(6) MILLER, K. J. and IBRAHIM, M. F. E. (1981) Damage accumulation during initiation and short crack growth regimes, *Fatigue Engng Mater. Structures*, **4**, 263–277.
(7) SEKI, M., TANAKA, T., and DENOH, S. (1971) Estimation of the fatigue life under programme load including the stresses lower than endurance limit, *Bull. Jap. Soc. mech. Engrs*, **14**, 183–190.
(8) MISAWA, H. and KODAMA, S. (1981) Fatigue crack propagation behaviour by cyclic overstressing and understressing, *Mem. Fac. Tech., Tokyo Metropolitan University*, No. 31, 2967–2980.
(9) CORTEN, H. T. and DOLAN, T. J. (1956) Cumulative fatigue damage, *Proc. Int. Conf. Fatigue of Metals* (Institution of Mechanical Engineers, London), pp. 235–246.
(10) MARSH, K. J. (1965) Cumulative fatigue damage under a symmetrical sawtooth loading programme, *Mech. Engng Sci.*, **7**, 138–151.
(11) DE LOS RIOS, E. R., MOHAMED, H. J., and MILLER, K. J. (1985) A micromechanics analysis for short fatigue crack-growth, *Fatigue Fracture Engng. Mater. Structures*, **8**, 49–63.
(12) MILLER, K. J., MOHAMED, H. J., and BROWN, M. W. (1985) A new fatigue facility for studying short fatigue cracks, *J. Fatigue Fracture Engng Mater. Structures*, in press.
(13) MILLER, K. J. (1985) Initiation and growth rates of short fatigue cracks, *Fundamentals of deformation and fracture* (Eshelby Memorial Symposium) (Cambridge University Press, Cambridge), pp. 477–500.
(14) HOBSON, P. D. (1986) *The growth of short fatigue cracks in a medium carbon steel*, PhD thesis, University of Sheffield.
(15) MOHAMED, H. J. (1986) *Cumulative fatigue damage under varying stress range conditions*, PhD thesis, University of Sheffield.
(16) ILETT, C., SOMEKH, M. G., and BRIGGS, G. A. D. (1984) Acoustic microscopy of elastic discontinuities, *Proc. R. Soc. London*, **A393**, 171–183.
(17) MILLER, K. J., MOHAMED, H. J., BROWN, M. W., and DE LOS RIOS, E. R. (1986) Barriers to short fatigue crack propagation at low stress amplitudes in a banded ferrite–pearlite structure, TMS-AIME, Santa Barbara meeting, to be published.
(18) MILLER, K. J. (1986) Introductory lecture, *Fatigue of engineering materials and structures*, Sheffield (Institution of Mechanical Engineers, London).